

EFFECT OF Co SUBSTITUTION ON MAGNETIC AND MAGNETORESISTANCE EFFECT IN $\text{La}_{0.67}(\text{Ba}_{1-x}\text{Co}_x)_{0.33}\text{MnO}_3$ SYSTEM

J.K.Wong, K.P.Lim, S.A. Halim, S.K. Chen and S.W. Ng

*Physics Department , Faculty of Science, University Putra Malaysia,
43400 UPM Serdang, Selangor, Malaysia*

ABSTRACT

A series of polycrystalline perovskite manganite of $\text{La}_{0.67}(\text{Ba}_{1-x}\text{Co}_x)_{0.33}\text{MnO}_3$ ($x=0.00$, 0.30 and 0.50) were prepared by conventional solid-state route. XRD spectrum indicates that single phase rhombohedral perovskite structure had been obtained for $x=0.00$ sample. When Co is introduced in the Ba site, its structure is distorted from rhombohedral to pseudo-cubic. The SEM images show that the average grain sizes were found to be in $3\text{-}8\mu\text{m}$ ($x=0.30$) and $2\text{-}10\mu\text{m}$ ($x=0.50$) with less pore between the grain. For $x=0.00$, the sample is found in melted condition where no significant clear grain boundary can be found. Pure sample had T_C of 343K . However, substitution of Co at Ba site brings down the Curie temperature, T_C below 293K . Pure ($x=0.0$) sample shows Low Field Magnetoresistance (LFMR) effect and the effect weakens when Co is introduced. The highest low-field MR value is -13.0% for sample with $x=0.00$ in 0.1Tesla applied external magnetic field at 90K and the highest MR value of -22.5% is given by $x=0.30$ sample at 1Tesla applied magnetic field at 90K . Hence, these indicated that Co will not enhance the extrinsic MR which is due to the grain boundary effect and tend to destroy the LFMR effect.

INTRODUCTION

The discovery of the colossal magnetoresistance (CMR) effect [1,2], where hole-doped polycrystalline manganites $\text{R}_{1-x}\text{A}_x\text{MnO}_3$ (R = rare-earth ions, A = divalent ions) with perovskite structure have been focused [3]. It is well know that interaction between $\text{Mn}^{3+}\text{-O-Mn}^{4+}$ mechanism of CMR in $\text{R}_{1-x}\text{A}_x\text{MnO}_3$ is explained by the double-exchange (DE) interaction [4,5]. However, DE interaction alone is not sufficient to explain the whole phenomena. It is suggested that lattice distortion due to the Jahn–Teller (JT) effect [6] is used to explain the magnetic and transport mechanisms in mixed-valence manganites. JT effect involved in the stretching modes of Mn^{3+} ions which splitting the e_g electronic level. In most cases, the large resistance changes are achieved only in a strong magnetic field of Tesla range and severely limit their practical applications. In general, most manganites compound having MR effect show maximum MR value near T_C or T_p . However, polycrystalline manganites compound also show a Low-field Magnetoresistance (LFMR) effect, known as extrinsic MR effect [7]. This effect shows a dramatic drop in the resistance when low magnetic field was applied. This is believed to be due to the spin-polarized tunneling or spin-dependent scattering across the grain boundaries [8]. In this work, the effect of Co substitution in Ba site for $\text{La}_{0.67}(\text{Ba}_{1-x}\text{Co}_x)_{0.33}\text{MnO}_3$ system had been studied.

METHODOLOGY

High purity of MnCO_3 , La_2O_3 , BaCO_3 , and Co_3O_4 (purity >99.5%) were used to prepare bulk polycrystalline sample of $\text{La}_{0.67}(\text{Ba}_{1-x}\text{Co}_x)_{0.33}\text{MnO}_3$ $x = 0.00, 0.30$ and 0.50 through the conventional solid state reaction technique. Wet milling with acetone was introduced to break down the agglomeration of initial starting powder. Then, the wet powders were dried and ground before calcination (900°C for 12 hours) take place. Bulk samples were reground and sieved in the range between $25\text{-}38\mu\text{m}$ to enhance the homogeneity of the grain size distribution and pressed into pellets before sintering at 1300°C for 24 hours. The crystal structure of synthesized samples was characterized by X-ray diffraction (XRD, Phillips PW 3040/60 Xpert Pro) technique with radiation of CuK_α ranging from 20° to 80° . The electrical properties of the bulk were characterized with four point probe technique at temperature of 90K to 300K in the external applied magnetic field up to 1 Tesla. Magnetic properties were measured by Vibrating Sample Magnetometer (VSM, Lakeshore 7400 series) at 303K up to 393K. Surface morphology was investigated by Scanning Electron Microscope (SEM, LEO1455 VPSEM).

RESULTS AND DISCUSSION

Figure 1(a) shows the XRD spectra of $\text{La}_{0.67}(\text{Ba}_{1-x}\text{Co}_x)_{0.33}\text{MnO}_3$ (LBCMO) sample. The spectrums reveal that all samples show similar pattern when referred to ICDD standards (ICDD NO: 01-089-0570) which indicated that single phase compound with rhombohedral structure had been obtained. Figure 1(b) shows the ($32^\circ\sim 33^\circ$) peak for all samples where it shifted to higher value and splitting when higher doping is introduced. The value of d-spacing is clearly influenced by the difference of Ba and Co average ionic radius, $\langle r_a \rangle$ (ionic radius of Ba^{2+} is 1.35\AA and Co^{2+} is 0.74\AA) which reduce the d-spacing. Since d-spacing is inversely proportional to $\sin \theta$ ($d \approx 1/\sin \theta$), the shifting of the peaks to higher 2θ value are reasonable. Splitting of the diffraction peaks occur with increasing x indicating that second phase might be formed at high substitution of Co into Ba. It is found that LBCMO ($x=0.00$) having single phases with rhombohedral structure while LBCMO ($x=0.50$) might certain some second phases. The main phase has rhombohedral structure followed by the pseudo-cubic phases when x increases. The connection of MnO_6 octahedron in the perovskite compound was tilted and distorted to form second phase in the material due to doping effect. This result is similar as reported earlier by other researcher [9].

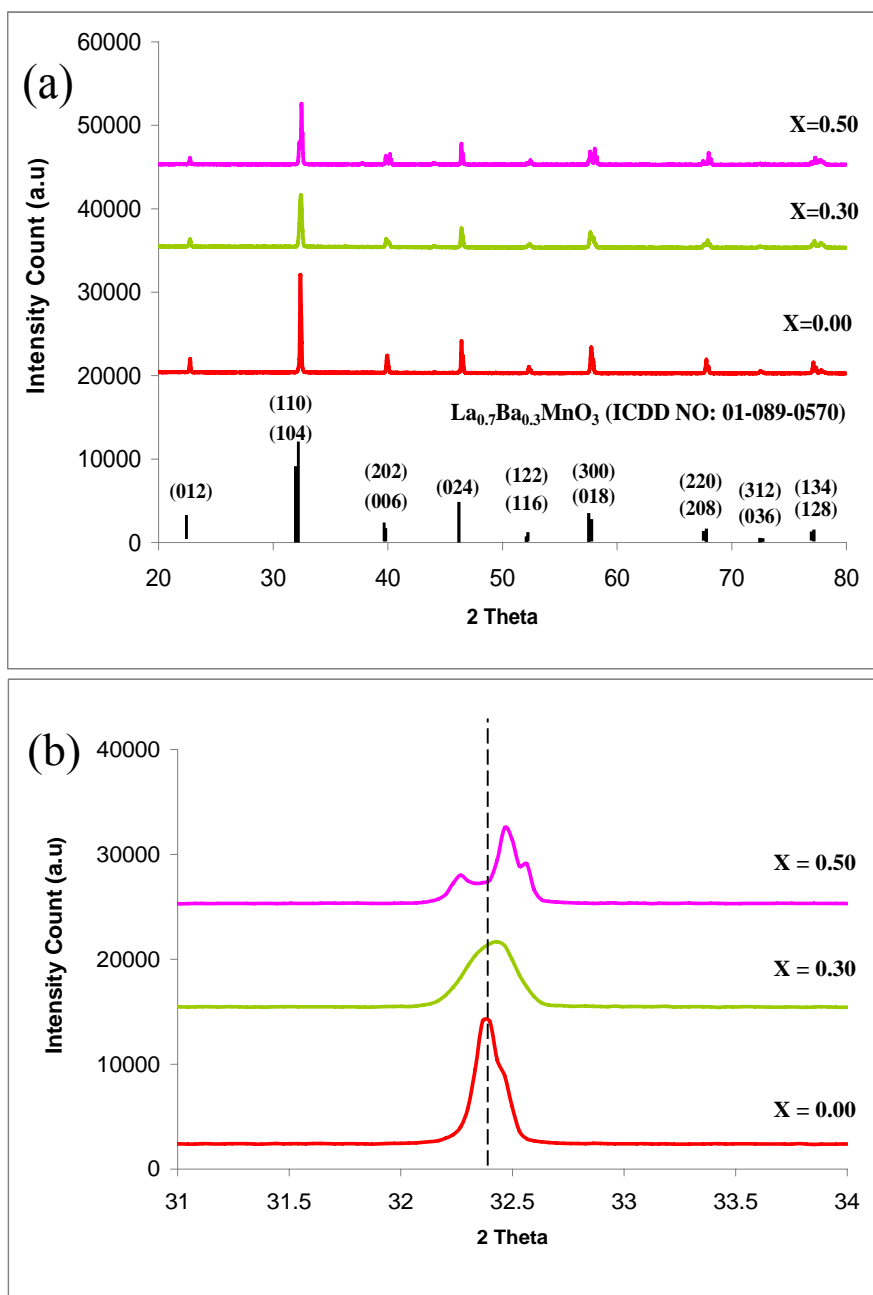


Figure 1: XRD spectrum of LBCMO compound with $x=0.00$, 0.30 and 0.50 (a) 20° to 80° and (b) 31° to 34° .

Figure 2 shows the SEM images of all samples. Clear grain is observed for sample $x=0.30$ and 0.50 with the average grain sizes of $3\text{-}8\mu\text{m}$ for $x=0.30$ and $2\text{-}10\mu\text{m}$ for $x=0.50$ except in the case of $x=0.00$. During sintering process, strong diffusion might occur for sample $x=0.00$ where the entropy of the system increase. Hence the compounds melt and no clear boundary is observed. All the particles are well

connecting with pore is observed between them. For $x=0.30$ and 0.50 , both sample show a grain boundary with no clear pore is observed. Hence, sample $x=0.30$ and $x=0.50$ is much more compact as compared to $x=0.00$. Meanwhile, Figure 2(b) and 2(c) further confirm the existing of second phases in the material. It shows the existing of different shape of grain in the material as marked circle in the figure (octahedral like microstructure with smooth and flat surface). This might correspond to pseudo-cubic phase as discussed in the XRD result.

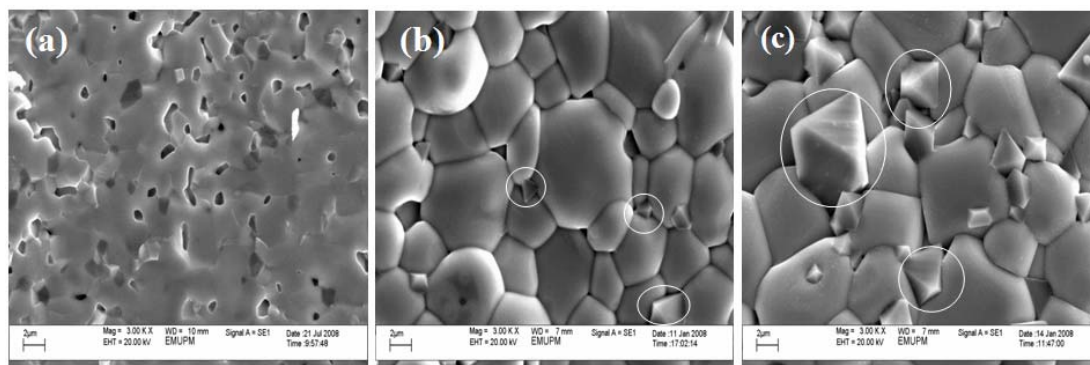


Figure 2: SEM images of LBCMO (a) $x=0.00$, (b) $x=0.30$ and (c) $x=0.50$.

The percentage of magnetoresistance (MR) is calculated using $MR\% = \frac{\rho_{(0)} - \rho_{(H)}}{\rho_{(0)}} \times 100$, where $\rho_{(0)}$ and $\rho_{(H)}$ is the resistivity at zero magnetic field and in an applied external magnetic field respectively. Sample with $x=0.00$ shows two obvious regions of %MR curve with different gradient, a sudden drop of MR in low magnetic field (<0.1 Tesla) region and followed by an almost saturation in higher magnetic field (>0.1 Tesla) region in all temperature. The initial drop of %MR is known as Low Field Magnetoresistance effect (LFMR) as shown in Figure 3(a). When low magnetic field was applied, the spin at the grain boundaries begin to align drastically. Thus, this will enhance the electron hopping by reduce the resistance according to DE theory. When stronger external magnetic field was applied (>0.1 Tesla), the spin in the core begin to align and causes further drop in resistance. Since LFMR effect is governed by the spin-polarized tunneling and spin-dependent scattering across the grain boundaries. The physical or connection between grains will influence the MR.

From Figure 3(a) and 3(b), substitution Co into Ba weakens and the Low Field Magnetoresistance (LFMR) effect vanish. These phenomena can be explained by considering the connectivity between grains. Since sample with $x=0.00$ is in the melted condition and no clear grain boundaries were observed, the spacing between grains are greatly small. As amount of Co substitute to Ba site increased (when $x=0.30$ and 0.50), formation of grain boundary is obvious and indicating that spacing between those grains might be thick. The spacing between grains will influence the flowing of electrons especially electrons that tunneling among grain boundaries. More energy is required for electrons to overcome the surface work function which act as an electron binder on

surfaces and the distance between two grains. In other words, melted compound ($x=0.00$) exhibit a very thin layer space among grains while a clear grain boundary compound which observed in the sample ($x=0.30$ and 0.50) have greater spacing compared to sample with $x=0.00$. Therefore, the LFMR effect had been weakened or destroyed corresponding to the increases of Co.

The maximum %MR values obtained are -22.5% followed by -20.0% and -17.7% at 90K in 1 Tesla field for sample with $x=0.30$, 0.00 and 0.50 respectively. At room temperature, % MR values are -9.1%, -13.5% and -15.2% in 1 Tesla applied external magnetic field when $x=0.00$, 0.30 and 0.50 respectively. The highest low-field MR value is -13.0% for sample with $x=0.00$ in 0.1Tesla applied external magnetic field at 90K. The increasing of %MR value due to the substitution of A-site with smaller ionic radius compound was similar as reported by Padmavathi et al [10].

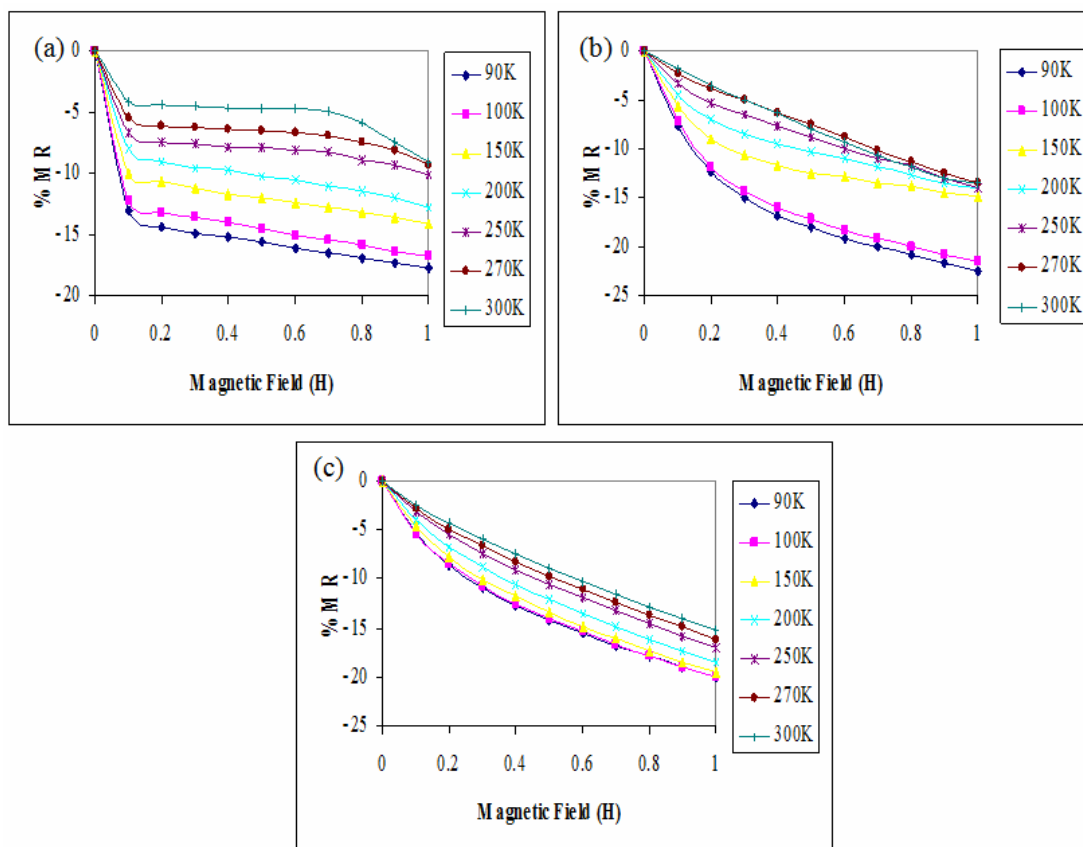


Figure 3: %MR curves as a function of applied external magnetic field at various temperature of LBCMO (a) $x = 0.00$, (b) $x = 0.30$ and (c) $x = 0.50$

Figure 4(a) shows the magnetization versus temperature for LBCMO in the range of 303K to 393K. Sample with $x=0.00$ shows a significant transition of ferromagnetic to paramagnetic which is known as Curie temperature, T_C . Samples with $x=0.30$ and 0.50 showed a linear line through the temperature range. The T_c might be shifted to lower

temperature as Co concentration increases. The derivative graph as in Figure 4(b) shows that the Curie temperature for pure sample is 343K which is greater than that as reported by Venkataiah et al. [11]. However, the doping of Co greatly reduces the magnetization value. Hence, the presence of Co could have disturbed the magnetic domain alignment at higher temperature.

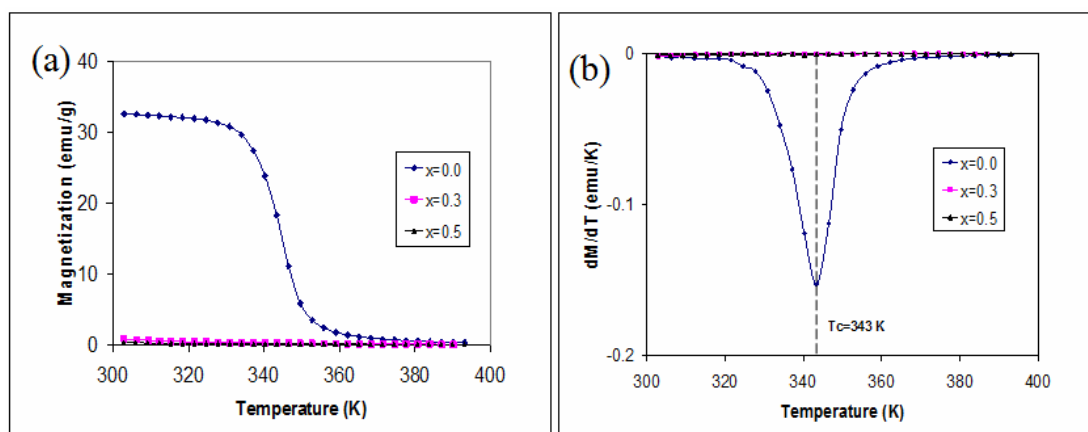


Figure 4: (a) Magnetization versus temperature for LBCMO and (b) Derivative of magnetization versus temperature for LBCMO.

CONCLUSION

As a conclusion, the system of $\text{La}_{0.67}(\text{Ba}_{1-x}\text{Co}_x)_{0.33}\text{MnO}_3$ ($x = 0.00, 0.30$ and 0.50) the effect of Co doping lead to the shrinkage of resulting in the formation a second phase. The replacement of Ba with Co gives larger range of grain size distribution. The average grain size range is found to be in $3\text{-}8\mu\text{m}$ ($x=0.30$) and $2\text{-}10\mu\text{m}$ ($x=0.50$) ranges while for pure sample a melt condition morphology was observed. LFMR effect had been weakened or vanished and the magnetic phase transition temperature, T_C reduces when Co is replaced with Ba. The Curie temperature for pure sample is 343K and greatly reduced below 300K when $x=0.30$ and 0.50 . T_C is shifted below room temperature while the magnetization value is greatly reduced. The highest %MR value is -22.5% when $x=0.30$ in 1Tesla applied external magnetic field at 90K and the highest low-field MR value is -13.0% for sample with $x=0.00$ in 0.1Tesla applied external magnetic field at 90K.

ACKNOWLEDGMENT

The Ministry of science, technology and Innovation of Malaysia is gratefully acknowledged for the grant under Science Fund vote: 03-01-04-SF0088: Fabrication of Multilayers Manganite Thin Film having LFMR Effect Using Pulsed Laser Ablation Technique.

REFERENCES

- [1]. S. Jin, T.H. Tiefel, M. McCormack, R.A. Fastnacht, R. Ramesh, L.H. Chen (1994). Thousandfold Change in Resistivity in Magnetoresistive La-Ca-Mn-O Films. *Science* **264**, 43.
- [2]. Y. Tokura, Y. Tomioka, H. Kuwahara, A. Asamitsu, Y. Moritomo, M. Kasai (1996). Magnetic field induced insulator-metal phenomena in perovskite manganese oxides. *Physica C* **263**, 544-549.
- [3]. Y. Tokura, Y. Tomioka (1999). Colossal magnetoresistance manganites. *Journal of Magnetism and Magnetic Materials* **200**, 1-23.
- [4]. C. Zener (1951). Interaction between the d-Shells in the Transition Metals. II. Ferromagnetic Compounds of Manganese with Perovskite Structure. *Physics Review* **82**, pg.403.
- [5]. A.J. Millis, P.B. Littlewood, B.I. Shraiman (1995). Double Exchange Alone Does Not Explain the Resistivity of $\text{La}_{1-x}\text{Sr}_x\text{MnO}_3$. *Phys. Rev. Lett.* **74**, 5144-5147.
- [6]. A.J. Millis, B.I. Shraiman, R. Mueller (1996). Dynamic Jahn-Teller Effect and Colossal Magnetoresistance in $\text{La}_{1-x}\text{Sr}_x\text{MnO}_3$. *Phys. Rev. Lett.* **7**, 175-178.
- [7]. M. Garcia Hernandez, A. de Andres, J.L. Martinez, D. Sanchez Soria, L. Martin Carron, and S. Taboada (2003). Transport properties and magnetoresistance of La-Ca manganites near the optimal doping concentrations. *Journal of Solid State Chemistry* **171**, 76-83.
- [8]. H.Y. Hwang, S.W. Cheong, N.P. Ong, B. Batlogg (1996). Spin-Polarized Intergrain Tunneling in $\text{La}_{2/3}\text{Sr}_{1/3}\text{MnO}_3$. *Phys. Rev. Lett.* **77**, 2041.
- [9]. K.X. Jin, C.L. Chen, S.L. Wang, S.G. Zhao, Y.C. Wang, Z.M. Song (2005). Structure and electrical properties in $\text{La}_{0.67}(\text{Ca}_{1-x}\text{Sr}_x)_{0.33}\text{MnO}_3$ films. *Material Science and Engineering B* **119**, 206-209.
- [10]. K. Padmavathi, G. Venkataiah, P. Venugopal Reddy (2007). Electrical behaviour of some rare-earth-doped $\text{Nd}_{0.33}\text{Ln}_{0.34}\text{Sr}_{0.33}\text{MnO}_3$ manganites. *Journal of Magnetism and Magnetic Materials* **309**, 237-243.
- [11]. G. Venkataiah, V. Prasad, P. Venugopal Reddy (2007). Influence of A-site cation mismatch on structural, magnetic and electrical properties of lanthanum manganites. *Journal of Alloys and Compounds* **429**, 1-9.